

Influence of Mn²⁺ Magnetic Ions on the Properties of Cd_{1-x}Mn_xS Thin Films Synthesized by Chemical Bath Deposition

A.E. Mali^{1,*}, A.S. Gaikwad¹, S.V. Borse², R.R. Ahire³

¹ Department of Physics, SPDM College, Shirpur, Dist. Dhule (MS) 425405, India

² Department of Physics, SSVPS College, Shindkheda, Dist. Dhule (MS) 425406, India

³ Department of Physics, SG Patil College, Sakri, Dist. Dhule (MS) 424304, India

(Received 26 November 2020; revised manuscript received 15 February 2021; published online 25 February 2021)

II-VI semiconductor based ternary CdMnS compound material has received more attention due to its wide area of applications in semiconductor technology. Cd_{1-x}Mn_xS ($x = 0, 0.2, 0.4, 0.6, 0.8$ and 1.0) thin films were successfully prepared by chemical bath deposition technique on non-conducting glass substrates. Thin films were deposited at a bath temperature of 80 °C and pH = 11 by using the chemical bath reaction of cadmium chloride (CdCl₂) and manganese chloride (MnCl₂) with thiourea (NH₄)₂S in an aqueous solution. Further, the prepared samples were characterized by UV-visible spectroscopy, photoluminescence, XRD, SEM and EDAX to study the optical, structural, surface, and chemical properties. Effect of Mn²⁺ ions on the film thickness of Cd_{1-x}Mn_xS films was investigated using weight difference technique. The film thickness of Cd_{1-x}Mn_xS films decreases as Mn²⁺ ions increase in the bath solution. The polycrystalline nature with hexagonal and cubic structures of the as-deposited films was confirmed by XRD. The band gap value of the deposited films was observed to increase with increasing Mn²⁺ ion concentration, this might be ascribed to the fact that Cd atom was substituted by Mn atom in the CdS structure. EDAX analysis confirmed the deposition of Cd, Mn and S elements in the films. Photoluminescence spectra of Cd_{1-x}Mn_xS with different values of the composition parameter x exhibited two emission peaks with different intensities. The measurement of the electrical resistivity of Cd_{1-x}Mn_xS films was performed at room temperature using two probe methods. The variation in electrical resistivity values with compositional parameters was discussed based on deposition parameters. The investigated polycrystalline Cd_{1-x}Mn_xS thin films show promising technological applications in semiconductor industry.

Keywords: CdMnS films, Optical properties, Electrical properties, Chemical bath deposition, Mn²⁺ ion.

DOI: [10.21272/jnep.13\(1\).01004](https://doi.org/10.21272/jnep.13(1).01004)

PACS numbers: 68.55.ag, 68.55.jd, 81.16.Be, 68.37.Hk, 78.66.Hf

1. INTRODUCTION

The n -type CdS [1] (band gap ~ 2.42 eV) and p -type MnS [2] (band gap ~ 3.88 eV) are important materials of group II-VI semiconductors and they have potential application prospect in electronics and optoelectronic devices, sensors, lasers and thin film based devices in semiconductor industries [3]. The CdS structure has high electrical resistivity values and the energy gap of CdS is narrow [4]. Hence, the use of CdS alone is not enough for future hopes. To do this, unlike earlier reports, we have incorporated here Mn²⁺ ions into the CdS structure to produce CdMnS thin films in a wide range of composition ($x = 0.0$ to 1.0). Doping of CdS with Mn²⁺ ions has been made to achieve improved structural, electrical and optical properties. Most of the research done so far has focused extensively on structural, optical and electrical properties of Cd_{1-x}Mn_xS thin films. However, the study of the influence of Mn²⁺ ions on various properties of Cd_{1-x}Mn_xS thin films is rare in the literature.

A variety of techniques like spray pyrolysis, thermal evaporation, molecular beam epitaxy, sputtering, chemical vapor deposition, pulsed laser deposition, chemical bath deposition (CBD) etc. have been used in the synthesis of CdMnS thin films [5, 6]. Among these, CBD is one of the important techniques. CBD can provide simplicity, cost effectiveness, ease of handling and requires low cost equipment. It can be performed using a range of precursors and synthesis conditions like

temperature, time, concentration of reactants etc. The technique is simple, inexpensive and has a high yield, reproducible on large-area thin films [7, 8].

This paper attempts to use a CBD technique for the deposition of Cd_{1-x}Mn_xS thin films for different values of the composition x and systematic study of the influence of Mn²⁺ ions on various characterization properties of Cd_{1-x}Mn_xS thin films.

2. EXPERIMENTAL DETAILS

Cd_{1-x}Mn_xS thin films were deposited using CBD technique. Cadmium chloride (CdCl₂), manganese chloride (MnCl₂) and thiourea (CH₄N₂S) were used as Cd²⁺, Mn²⁺ and S²⁻ ion sources, respectively. The stock solutions of CdCl₂ (1 M), MnCl₂ (1 M) and thiourea (1 M) all of AR grade were prepared using distilled water. The experimental solutions of CdCl₂ and MnCl₂ were dissolved in high purity DI water in 50 ml glass beaker. Subsequently, thiourea was added dropwise to the solution with continuous stirring until a volume of 50 ml reached. Ammonia solution was added until the pH reached 11 and stirred for few minutes. The microscopic non-conducting glass substrate was cleaned with distilled water and liquid soap, soaked in dilute HCl for one day, washed with acetone and finally with distilled water. Then the substrate was kept vertically inclined into the chemical bath. The chemical bath maintained at 80 °C for one hour. Finally, deposited samples were taken out of the solution cleaned with DI water and

* aemalispdm@gmail.com

dried in air at room temperature. To study the influence of Mn^{2+} on various properties of $Cd_{1-x}Mn_xS$ thin films, the CBD parameters, such as complexing agent, deposition time, temperature and pH of the solution were firstly optimized in the present procedure to achieve good quality films. Fig. 1 shows the schematic sketches of the sample preparation process.

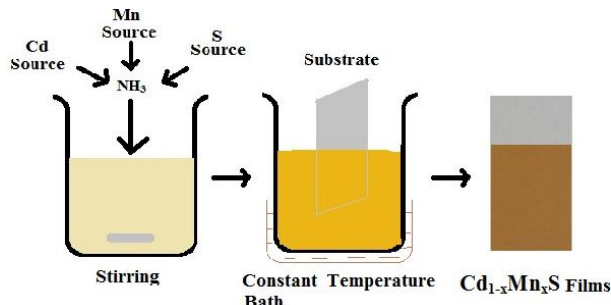
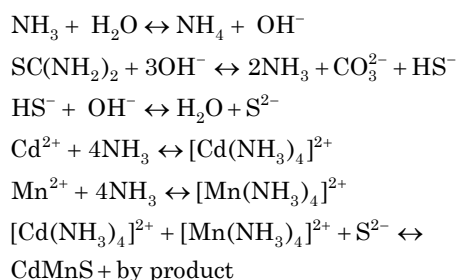


Fig. 1 – Process flow for deposition of $Cd_{1-x}Mn_xS$ films

The deposited CdMnS thin film exhibits yellowish to yellow brownish color with variation in Mn^{2+} ion concentration.

The chemical reaction for the deposition of CdMnS by CBD is as shown below



3. RESULTS AND DISCUSSION

The as-deposited films were characterized by different techniques. The film thickness was measured using gravimetric weight difference method. The XRD of the films was recorded using Bruker AXS D8 advance spectrophotometer. The surface morphology of the CdMnS films was analyzed by FESEM (SEM Hitachi S-47009). The compositional purity of the films was confirmed by EDAX analysis. The UV-visible spectrum was recorded by the spectrophotometer in the wavelength range 300-900 nm. The room temperature PL spectrum was recorded by Perkin Elmer LS55 using laser source at a wavelength of 390 nm. The dc electrical transport properties have been studied at room temperature by two-probe dc electrical conductivity equipment.

3.1 Thickness Measurement

The as-deposited film thickness of $Cd_{1-x}Mn_xS$ samples was measured by gravimetric weight difference method using a high-precision electric balance. This method gives an appropriate value of the thickness of the deposited films. The thickness of the film can be determined using the equation [9]

$$t = \frac{(w_2 - w_1)}{A\rho} \times 10^{-4} \text{ } \mu\text{m}$$

where w_1 and w_2 are the weights of the substrate before and after film deposition in grams, A is the area of the deposited film in cm^2 and ρ is the theoretical density of the deposited material.

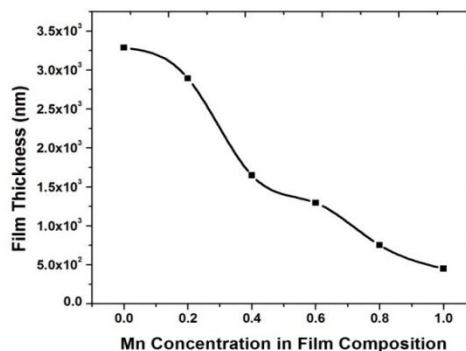


Fig. 2 – Variation in film thickness as a function of Mn concentration

Fig. 2 shows the variation in film thickness versus Mn^{2+} ion concentration in the CdS structure. It is seen that the thickness of the film decreases with the addition of Mn^{2+} ions to the CBD solution. It can be ascribed to the fact that Mn^{2+} ion has smaller atomic/ionic radius (117/80 Pm) than that of Cd^{2+} (154/97 Pm). As Mn^{2+} ion concentration in the bath solution increases, the film (Mn^{2+}) content also increases. Further, substitution of Cd^{2+} by Mn^{2+} atoms is easily possible in the chemical bath.

3.2 Characterization Using XRD

The crystal structure of the as-deposited films has been investigated by XRD patterns which are shown in Fig. 3. The diffractogram illustrated in the figure clearly shows that the as-deposited films are polycrystalline in nature. The analysis of these diffractograms was done and the corresponding data (interplanar distance d , hkl planes, grain size etc.) were determined. There are six prominent reflections at d values equal to 3.577 Å, 3.351 Å, 3.164 Å, 2.066 Å, 1.890 Å and 1.760 Å that correspond to the (100), (002), (101) (110), (103) and (200) reflections, respectively. XRD pattern of the films indicates that they are polycrystalline with both the hexagonal wurtzite type structure (JCPDS card No. 772306 for CdS and card No. 894953 for MnS) and cubic structure with preferential growth along the (002) direction. The addition of Mn^{2+} to the CdS matrix showed the formation of a solid solution up to $x = 0.8$. The further incorporation of Mn^{2+} resulted in phase separation of both CdS and MnS.

The average grain size enhanced with the addition of Mn^{2+} ions into the bath solution. A plot showing grain size versus concentration is represented in Fig. 4. When Mn^{2+} ions are added to the host lattice of CdS, Mn atoms substitutionally occupy Cd atom sites instead of forming a separate MnS phase. The effect of Mn^{2+} ions on grain size of the obtained films is shown in Fig. 4.

This caused improved crystallinity, especially for $x = 0.2$. Above the composition $x = 0.4$, phase separation started resulting in deterioration of crystallinity for films with $x = 0.6$ and $x = 0.8$. Films with $x = 1.0$ represent amorphous nature with dominant MnS phase [10].

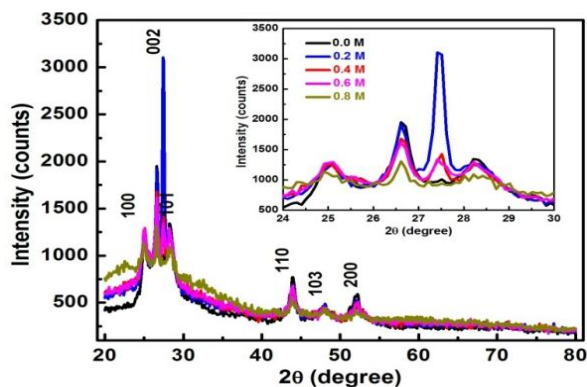


Fig. 3 – X-ray diffraction spectra of CdMnS films. The inset shows intense peaks

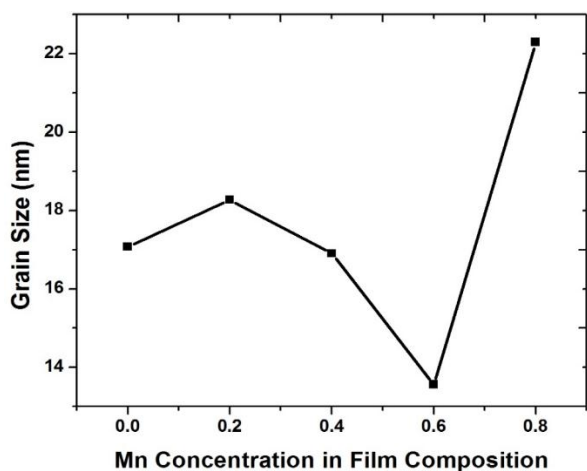


Fig. 4 – Effect of Mn concentration in the film composition on grain size

Table 1 – Observed and standard 2θ and d values for respective hkl planes

Sr. No.	2θ , degrees		d , Å		Planes (hkl)
	Observed	Standard	Observed	Standard	
1	24.90	25.18	3.5775	3.5380	(100)
2	26.61	26.91	3.3514	3.3147	(002)
3	28.21	28.61	3.1648	3.1215	(101)
4	43.84	44.36	2.0660	2.0430	(110)
5	48.15	48.60	1.8906	1.8716	(103)
6	51.96	51.69	1.7606	1.7692	(200)

The XRD data are given in Table 1. The average grain size in the deposited films is estimated using Scherrer relation:

$$D = \frac{k\lambda}{\beta \cos\theta}, \quad (2)$$

where k is the Scherrer constant, λ is the wavelength of X-rays, β is the full width at half maximum (FWHM) in radians and θ is the Bragg angle.

3.3 SEM Analysis

The surface morphology of $Cd_{1-x}Mn_xS$ thin films was investigated by FESEM. Fig. 5 shows variations in the surface morphology of $Cd_{1-x}Mn_xS$ ($x = 0.0, 0.2, 0.4,$

$0.6, 0.8, 1.0$) films with respect to increase in Mn^{2+} ion concentration in the coating solution. All the films were scanned at 20 K magnification.

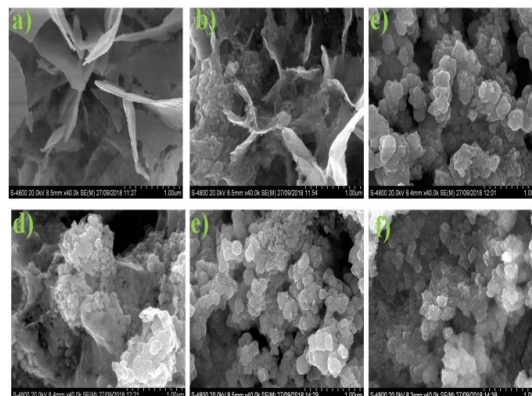


Fig. 5 – FESEM images of the films: a) CdS, b) $Cd_{0.8}Mn_{0.2}S$, c) $Cd_{0.6}Mn_{0.4}S$, d) $Cd_{0.4}Mn_{0.6}S$, e) $Cd_{0.2}Mn_{0.8}S$, f) MnS

The micrographs show the uniform deposition of $Cd_{1-x}Mn_xS$ films without any pinholes. Pure CdS has a flower-like structure and is shown in Fig. 5a. As we incorporate Mn^{2+} ions into CdS coating solution, Mn atoms interact with CdS molecules. This interaction slightly changes the film surface morphology, which is confirmed by Fig. 5b. Further increase in Mn^{2+} ion concentration in the coating solution resulted in the formation of nanocrystalline CdMnS compounds that is shown in Fig. 5c-e. When concentration of Mn^{2+} ions reaches the highest level, Cd atoms are replaced by Mn atoms and this gives us the pure form of MnS films. The nanocrystalline morphology of pure MnS films is shown in Fig. 5f.

3.4 EDAX Analysis

To confirm the elemental composition of Cd, Mn and S in CdMnS thin films, EDAX is carried out. Table 2 shows EDAX data of the deposited $Cd_{1-x}Mn_xS$ ($x = 0.4$) thin films. It also confirms the presence of Cd^{2+} , Mn^{2+} and S^{2-} in the obtained film matrix.

Table 2 – EDAX data for $Cd_{1-x}Mn_xS$ ($x = 0.4$) films

Element	Atomic number	Series	Atomic percent (%)
S	16	K-series	42.22
Mn	25	K-series	17.26
Cd	48	L-series	40.52
Total			100

3.5 UV-visible Spectrophotometer

The optical absorbance data of CdMnS thin films were recorded using UV-visible spectrophotometer. The absorbance spectra were used to estimate the energy band gap (E_g) by Tauc plot method. It is found that the optical band gap has been enhanced with composition. This is shown in Fig. 6. With an increase in Mn^{2+} ions, the strain was induced by Mn^{2+} ions, and therefore the lattice structure became highly distorted tending towards amorphisity of the material that caused the band gap to be enhanced. This enhancement in the

band gap is in good agreement with previous results. The band gap values vary from 2.05 to 2.82 eV which is consistent with the values reported for thin films obtained by CBD [5, 11].

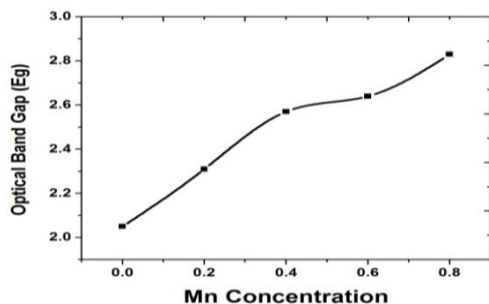


Fig. 6 – Effect of Mn concentration on band gap

The dependence of the optical band gap on the Mn^{2+} ion concentration can be attributed to Mn atoms in the CdS structure [12, 13]. The difference in the band gap values is clearly indicated by the color of the thin film, the yellow color turned to dark yellowish or orange color as Mn^{2+} ions increase.

3.6 Photoluminescence Analysis

Photoluminescence (PL) is an efficient, non-contact and non-destructive method to probe the electronic structure of different materials, which can also be used to determine the band gap, impurity levels, defects etc. Fig. 7 represents the room temperature PL spectra of $\text{Cd}_{1-x}\text{Mn}_x\text{S}$ thin films, showing two broad emission peaks at 525 and 589 nm. The emission peak at 525 nm corresponds to the green band; it is due to the donor-acceptor transition and is attributed to the radiative recombination of a hole in the valence band and of an electron in the conduction band. In addition, the unshifted peak positions indicate that the crystallite sizes are almost the same for all samples. Our XRD studies shed light on these observations. Another well-known emission peak at 589 nm (2.1 eV, red band) corresponds to the ${}^4\text{T}_1-{}^6\text{A}_1$ transitions of Mn^{2+} *d*-states in CdS nanocrystals.

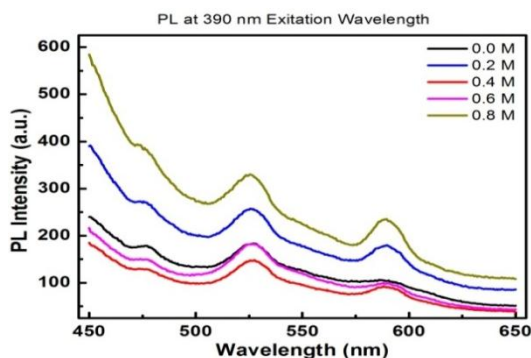


Fig. 7 – Photoluminescence spectra of CdMnS films

The vacancies created by Cd atom (surface defects) can either act as traps or as non-radiative recombination centers. Thus, PL analysis indicated that Mn^{2+} ions are distributed on the surface of the CdS lattice and fill the vacancies of Cd atoms.

3.7 Electrical Properties

The electrical resistivity of all CdMnS thin film structures was measured by two-probe method at room temperature. The electrical resistivity (ρ) of the sample has been determined using the relation

$$\rho = \frac{RA}{t} \quad (3)$$

where R is the resistance, t is the thickness, and A is the cross section area of the film. It is found that room temperature electrical resistivity has been enhanced with composition up to $x = 0.2$. For further increase in Mn^{2+} ions, room temperature electrical resistivity decreases.

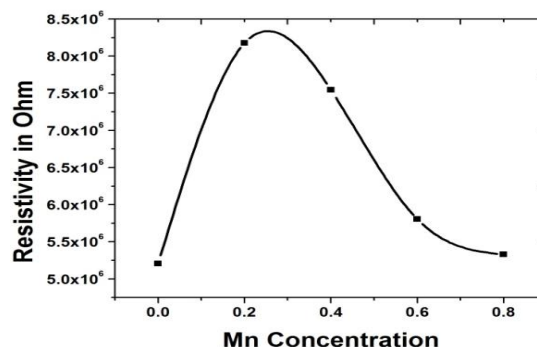


Fig. 8 – Effect of Mn concentration on resistivity of CdMnS films

This is shown in Fig. 8. The resistivity modulation by incorporation of Mn^{2+} ions into CdS lattice can be explained based on the following facts: Cd^{2+} and Mn^{2+} are co-deposited simultaneously and substitution of Cd^{2+} ions by Mn^{2+} is the predominant mechanism under this situation. The EDAX analysis of $\text{Cd}_{1-x}\text{Mn}_x\text{S}$ films also supported these observations. Also, as we add Mn^{2+} ions into CdS lattice, initially they do not react with CdS and do not form CdMnS alloy. Since the volume of Cd atom is greater than that of Mn atom, hence Mn^{2+} ions settle down at the interstitial sites of the CdS lattice. This, in turn, increases the number of scattering centers in the material, hence the resistivity. With further addition of Mn^{2+} to CdS lattice, some Mn atoms settle down at the interstitial sites of the CdS lattice, while other atoms form CdS as well as CdMnS. As a result, CdMnS dominates in the film, and hence the numbers of scattering centers reduces resulting in a decrease in resistivity. Thus, by the addition of Mn^{2+} ions into CdS films, resistivity values decrease. This property is more beneficial in designing solar cells.

4. CONCLUSIONS

The optimum condition with a bath temperature of 80 °C and pH ~ 1 yielded good quality thin films of $\text{Cd}_{1-x}\text{Mn}_x\text{S}$ using CBD technique. The effect of Mn^{2+} ion concentration on the optical, structural, morphological and electrical properties has been investigated by various analysis techniques. The structural characterization reveals the polycrystalline nature in mixed phases (hexagonal and cubic), and grain sizes are of the order of few nm. It is found that grain sizes are almost

the same for all $Cd_{1-x}Mn_xS$ thin films with variation in Mn^{2+} ion concentration. The optical study reveals the increase in the band gap value with Mn^{2+} incorporation. The electrical resistivity was found to be enhanced with x up to 0.2 and then decreased with further increase in Mn^{2+} ion concentration. The photoluminescence result confirms that Mn^{2+} ions induce luminescence, exhibiting two broad peaks at 525 and 589 nm. Surface morphology also confirms almost uniform grain size of the crystals. EDAX analysis of the films shows that as Mn^{2+} ion concentration changes, the films become almost stoichiometric. Overall, the obtained $Cd_{1-x}Mn_xS$ thin films demonstrate the potential for use as a promising material for technological applications.

ACKNOWLEDGEMENTS

REFERENCES

1. Woodhead Publishing Series in Electronic and Optical Materials, *Semiconductor Nanowires* (Ed. by J. Arbiol, Q. Xiong) (Woodhead Publishing: 2015).
2. C. Gümüş, C. Ulutaş, Y. Ufuktepe, *Opt. Mater.* **29** No 9, 1183 (2007).
3. R.N. Bhargava, *J. Cryst. Growth* **86**, 873 (1988).
4. L. Huang, Z.L. Wei, F.M. Zhang, X.S. Wu, *J. Alloy. Compd.* **648**, 591 (2015).
5. F. Iacomi, I. Salaoru, N. Apetroaei, A. Vasile, C.M. Teodorescu, D. Macovei, *J. Optoelectron. Adv. M.* **8**, 266 (2006).
6. H. Sekhar, G.T. Rao, P.H. Reddy, D.N. Rao, *J. Alloy. Compd.* **562**, 38 (2013).
7. J. Cheng, D. Fan, H. Wang, B. Liu, Y. Zhang, H. Yan, *Semicond. Sci. Technol.* **18** No 7, 676 (2003).
8. D. Mugle, G. Jadhav, *AIP Conf. Proc.* **1728**, 020597 (2016).
9. C. Lai, X. Li, C. Liu, X. Guo, Z. Xiang, B. Xie, L. Zou, *Mater. Sci. Semicond. Process* **26**, 501 (2014).
10. M.P. Gonullu, S. Kose, *Metall. Mater. Trans. A* **48** No 3, 1321 (2017).
11. S.M. Al-Jawad, *Int. J. Appl. Innov. Eng. Manag.* **3**, 329 (2014).
12. M. Ikeda K. Itoh, H. Sato, *J. Phys. Soc. Jpn.* **25**, 455 (1986).
13. C.T. Tsai, S.H. Chen, D.S. Chuu, W.C. Chou, *Phys. Rev. B* **54**, 11555 (1996).

This work was supported by University Grants Commission (UGC, WRO), India, under minor research project scheme (File No. 47-1066/14(WRO) dated 08/01/2016). Authors are thankful to the Principal, Dr. S.N. Patel, SPDM College, Shirpur for providing necessary college level facilities. Authors are also thankful to Dr. P.K. Baviskar, PostDoc Fellow, SPPU, Pune, who helped in various ways during this work.

AUTHOR CONTRIBUTIONS

Ashok E. Mali and Anil S. Gaikwad equally contributed in manuscript preparation, designing experimental setup, carrying out measurements and analysis part, Sanjay V. Borse and Rajendra R. Ahire contributed in composition of manuscript and result analysis.